Hindawi
Journal of Sensors
Volume 2019, Article ID 1312709, 16 pages
https://doi.org/10.1155/2019/1312709

Research Article

Soft Sensing Modeling of the SMB Chromatographic Separation Process Based on the Adaptive Neural Fuzzy Inference System

Dan Wang,[1] Jie-Sheng Wang,[1] Shao-Yan Wang,[2] Shou-Jiang Li,[2] Zhen Yan,[1] and Wei-Zhen Sun[3]

[1]*School of Electronic and Information Engineering, University of Science and Technology Liaoning, Anshan City, Liaoning Province, China*
[2]*School of College of Chemical Engineering, University of Science and Technology Liaoning, Anshan City, Liaoning Province, China*
[3]*Fujian Institute of Research on the Structure, Fujian Province, China*

Correspondence should be addressed to Jie-Sheng Wang; wang_jiesheng@126.com

Received 27 April 2019; Accepted 17 October 2019; Published 13 November 2019

Academic Editor: Jesús Lozano

Simulated moving bed (SMB) chromatographic separation technology is a new adsorption separation technology with strong separation ability. Based on the principle of the adaptive neural fuzzy inference system (ANFIS), a soft sensing modeling method was proposed for realizing the prediction of the purity of the extract and raffinate components in the SMB chromatographic separation process. The input data space of the established soft sensor model is divided, and the premise parameters are determined by utilizing the meshing partition method, subtractive clustering algorithm, and fuzzy *C*-means (FCM) clustering algorithm. The gradient, Kalman, Kaczmarz, and PseudoInv algorithms were used to optimize the conclusion parameters of ANFIS soft sensor models so as to predict the purity of the extract and raffinate components in the SMB chromatographic separation process. The simulation results indicate that the proposed ANFIS soft sensor models can effectively predict the key economic and technical indicators of the SMB chromatographic separation process.

1. Introduction

SMB chromatographic separation technology is a new separation technology developed on the basis of traditional fixed bed adsorption operation and true moving bed (TMB) chromatographic separation technology [1]. As the main modern adsorption separation technology, SMB chromatography has been utilized more and more in the complex mixture separation process, such as petrochemical, fine chemical, biopharmaceutical, and food processing. SMB chromatography technology is the cutting-edge technology in separation science, which preserves the high separation rate, low energy consumption, and low material consumption of the chromatogram. It also introduces the continuous, countercurrent, rectification, reflux, and other mechanisms of moving bed technology. Compared with the existing chemical separation technology (distillation, extraction, single-column chromatography), this technology can achieve automatic continuous separation, which can increase separation capacity and improve product yield, yield, and efficiency. It is the key technology for the chemical separation process and can also reuse the stationary phase and mobile phase to reduce cost and energy consumption [2]. In the cyclical operation of continuous production, the SMB system fully reflects its nonlinear, nonideal, and nonequilibrium characteristics. This multidegree-of-freedom system finds it difficult to make the important performance indicators, such as product purity, yield, and mobile phase consumption, in periodicity optimal states [3, 4].

The adaptive neural fuzzy inference system is an artificial intelligence inference technology with the advantages of fuzzy logic and neural network [5], which is a good nonlinear mapping technique. ANFIS can construct a clear input-output mapping structure, which provides a powerful learning and decision-making process for target systems including nonlinear systems and has been successfully applied in the

prediction of short-term electricity prices [6], clay expansion capacity [7], wind speed profile estimation [8], and the thermal error compensation on the CNC machine [9]. The ANFIS fuzzy neural network model was used to predict the cutting speed in WEDM [10]. The ANFIS model was used to predict the density of ionic liquids at various temperatures [11]. The particle swarm optimization (PSO) algorithm was used to obtain appropriate subtractive clustering (SC) parameter settings, and an adaptive ANFIS model was built to predict the business success rate [12]. ANFIS and artificial neural network (ANN) models were established for predicting the drying characteristics of potato, garlic, and cantaloupe in convection hot air dryers [13]. The polynomial equation of the bank section by utilizing the hybrid ANFIS was used to stabilize the design and implementation of the river section [14]. A data-driven model of the debutanizer based on ANFIS was established for realizing the real-time composition monitoring [15]. ANFIS was applied to develop an accurate temperature-dependent intelligent model for correlating the loading capacity of amino acid salt solutions for a variety of amino acids [16]. The combination of the ANFIS and CFD method provides the nondiscrete domain in various dimensions and makes a smart tool to locally predict multiphase flow [17]. The ANFIS prediction model was established for the response during the stainless steel 202 turning operation [18].

In this paper, an ANFIS-based soft modeling method for the SMB chromatography separation process was proposed, which lays a foundation for the SMB system to achieve the periodic optimum stable working condition. The structure of the paper is described as follows. Section 2 introduces the SMB chromatographic separation technique and the structure of the established soft sensor model. Three input data space partitioning methods and four conclusion parameter optimization algorithms of ANFIS are introduced in Section 3. Section 4 describes the experimental simulation and result analysis. Finally, the conclusion is listed in the last part.

2. SMB Chromatography Separation Technology and Soft Sensor Modeling

2.1. SMB Chromatography Separation Technology. SMB chromatographic separation technology simulates the reverse flow of a stationary phase adsorbent by continuously switching the positions of each feed and discharge port. The basic principle of typical SMB is described as follows. The several chromatographic columns are connected to form a loop. The relative countercurrent of the stationary phase and the mobile phase is simulated by orderly moving the eluent inlet, the extract outlet, the feed liquid inlet, and the raffinate outlet in the direction of the mobile phase so as to achieve the separation of two components [19]. Taking the separation of two components as an example, the working principle is briefly explained. The working principle of the typical SMB chromatographic separation process is shown in Figure 1 [20, 21]. It is assumed that two components to be separated are A and B, respectively. The adsorption capacity of component A is stronger than that of component B. D is the desorbent, E is the extract, F is the feed, and R is the raffinate. The entire bed can be divided into four zones (respectively, referred to as I, II, III, and IV or 1, 2, 3, and 4) depending on the location and function of the liquid inlet and outlet. Each zone performs a specific function.

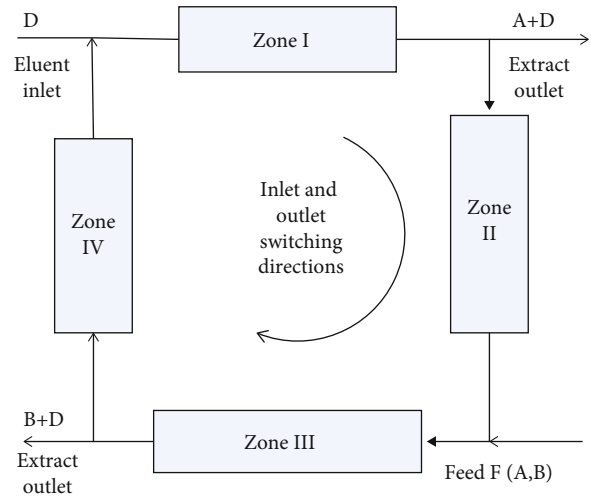

Figure 1: Working principle of the SMB cinematographic separation process.

Zone I. The strong adsorption component A was resolved from the stationary phase adsorbent by using desorbent D. The fresh desorbent enters from the bottom of zone I and contacts with the adsorbent, and component A is rinsed out and then discharged from the extract outlet at the top of the zone to obtain an extract.

Zone II. This is the analytical zone of weakly adsorbed component B. In the liquid entering zone II from zone I (including A and D), since component A has a stronger adsorption capacity than component B, component B in zone II is continuously displaced by component A and enters zone III along with the flowing liquid and the fresh feed (A and B).

Zone III. Strongly adsorbed component A is adsorbed by the adsorbent in this zone. B is discharged from the raffinate outlet through a liquid flowing downward to obtain the raffinate.

Zone IV. Its function is to achieve regeneration of eluent D and reduce the amount of eluent D. Since the concentration of D in zone IV is much higher than the concentration of D flowing into zone IV from the zone III region (because the region is zone I in the last switching cycle, eluent D is adsorbed by the adsorbent after being flushed with A, so its concentration is higher). Therefore, the adsorption equilibrium will be reestablished and eluent D will be resolved to achieve regeneration. The regenerated eluent D and the fresh eluent D flow into zone I together. In this way, the reverse flow of the stationary phase adsorbent is simulated by continuously switching the liquid inlet and outlet position in the switching direction shown in Figure 1, thereby achieving an effect equivalent to TMB.

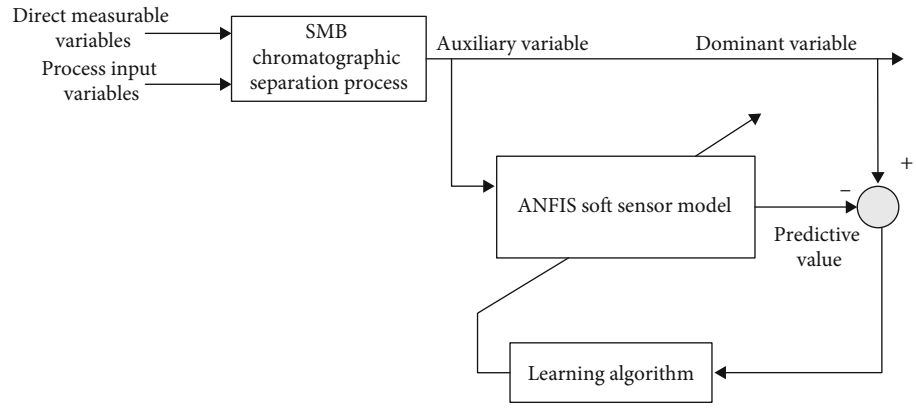

Figure 2: Structure of the soft sensor model.

The feeding and discharging ports divide the SMB flow system into different zones. For the SMB with three zones, the functions of each zone are described as follows.

Zone I. Elution zone: it desorbs the adsorbed substances on the stationary phase and flows out from the E port to complete the regeneration process of the stationary phase.

Zone II. Distillation zone: continuous elution with the mobile phase makes the fast and slow components further separated in the chromatographic column.

Zone III. Adsorption zone: the raw materials from the inlet flow into this zone and are adsorbed and separated, so that fast components flow out of the outlet (R port) of this zone and slow components are adsorbed in the stationary phase.

2.2. Soft Sensor Modeling for the SMB Chromatography Separation Process. In the SMB chromatography adsorption separation process, the purity of the product components in the extraction solution and raffinate is more important. However, the online measurement of the component purity as a quality index is difficult to achieve, and there are many factors affecting the product component purity in the SMB separation process. Therefore, the soft sensor modeling method for predicting the component purity in the SMB chromatography separation process has theoretical significance and application value [22]. The basic idea of soft sensing technology is to combine the automatic control theory with the knowledge of the production process. According to some optimal criteria, because some important variables are difficult to measure or temporarily unable to measure, the computer technology is used to select other variables that are easy to measure and to infer or estimate by constructing a mathematical relationship. The soft sensor model can be expressed as

$$\widehat{X} = f(d, u, y, X^*, t), \tag{1}$$

where $\widehat{X}$ is the dominant variable estimated value, d is the measurable disturbance, u is the control input variable, y is the measurable output variable, and X^* is the off-line sampled value or the analytically calculated value of the estimated variable. The optimal estimate of X can be obtained by constructing the relationship between these variables. Equation (1) reflects the relationship between the dominant variable X and the input variable u, the auxiliary variable y, and the measurable disturbance d_2, while the off-line sample value X^* is often used for self-correction of the model. The structure of the soft sensor model for the SMB chromatographic separation process established in this paper is shown in Figure 2.

The auxiliary variables in the soft sensor model are selected from the measurement variables that can be provided in the control system based on the technique mechanism of the production process. Based on the technique mechanism and prior knowledge of the SMB chromatography separation process, the following variables are selected as the auxiliary variables of the soft sensor model.

(1) Flow rate of the injection pump (F pump) of the raw material liquid inlet, whose unit is ml/min

(2) Flow rate of the flushing pump (D pump) of the flushing fluid inlet, whose unit is ml/min

(3) Valve switching time, whose unit is min

Select the following variables as the output variable of the established soft sensor model.

(1) The purity of the target in the effluent of the E port. If there is impurity at the E port, this purity is smaller than 1

(2) The purity of the impurity in the outlet effluent of the R port. If there is target material at the R port, this purity is smaller than 1

(3) Divide the mass of the target in the E port by the target injection quality so as to obtain the yield of the target at the E port

(4) Divide the mass of the impurity in the R port by the impurity injection quality so as to obtain the yield of the impurity at the R port

Table 1: Data of the SMB chromatography separation process.

Number	Feed concentration (mg/ml)	Flow rate of F pump (ml/min)	Flow rate of D pump (ml/min)	Switching time (min)	Purity of E port (%)	Purity of E port by simulated calculation (%)	Recovery of R port (%)	Recovery of R port by simulated calculation (%)
1	5.6	0.1	1.0	15.5	95	99.99	71	69.6
2	10	0.1	0.828	17	98.1	99.99	90	88.3
3	10	0.1	0.7	19	98.2	99.99	97.2	99.9
4	10	0.1	1.0	14.5	96.9	99.99	83	84.6
5	10	0.1	0.7	19.5	96	99.99	91	93.2
6	14.3	0.2	0.6	19	98.2	99.99	83	83.1
7	5.3	0.3	0.6	19.5	97.5	99.99	80	81
8	10	0.2	1.0	14.5	96.6	99.99	43	44.3
9	10	0.2	0.4	29	98.5	99.99	64	65.2
…	…	…	…	…	…	…	…	…
1000	10.4	0.2	0.7	19.5	95.7	99.99	48	46.1

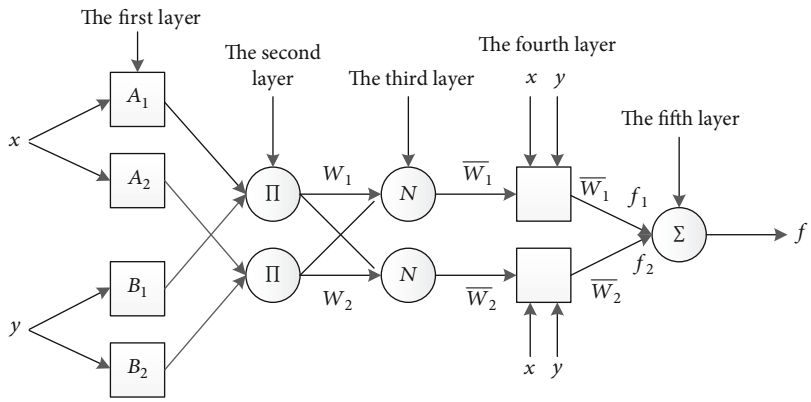

Figure 3: Structure diagram of typical ANFIS.

The auxiliary variables are used as inputs, and the purity of the target in the E port and the purity of the impurities in the R port are output variables. ANFIS is used to fit the nonlinear relationship among them so as to establish a predictive model of the corresponding economic and technical indicators. Based on a SMB chromatographic separation process, a soft sensor modeling method on the purity and yield of E and R ports is proposed by utilizing ANFIS. The historical data of the SMB chromatographic separation process were collected, and 1000 sets of historical data with uniformity and representative shown in Table 1 are selected as the modeling data. Before carrying out the soft sensor modeling with these data, it is necessary to perform data normalization shown in Equation (2) in order to eliminate the influence of variable unit on modeling accuracy.

$$y = \frac{x - v_{\min}}{v_{\max} - v_{\min}}, \tag{2}$$

where x is the initial value of the data set, y is the data after x being normalized, $v_{\max}$ is the maximum in the data set, and $v_{\min}$ is the minimum in the data set.

3. ANFIS and Training Algorithms

3.1. Basic Principles of ANFIS Based on Mesh Generation. In the early 1990s, Jang proposed an ANFIS based on the T-S model [5], which is a new type of neural network structure combining fuzzy theory. It uses a neural network to realize three basic processes of fuzzification part, fuzzy inference part, and defuzzification in fuzzy control so that the established system has the advantages of both theories and realizes the adaptive adjustment on the research object [23]. The typical structure of the ANFIS is shown in Figure 3. The prototype ANFIS adopts the meshing partition method to linearly divide the input space so as to determine the number of fuzzy rules [24].

Assume that the fuzzy inference system under consideration has two inputs x and y and a single output f. For the first-order Sugeno fuzzy model, the general rule set with two if-then rules is represented as follows.

Rule 1. If x is A_1 and y is B_1, then

$$f_1 = p_1 x + q_1 y + r_1. \tag{3}$$

Rule 2. If x is A_2 and y is B_2, then

$$f_2 = p_2x + q_2y + r_2. \tag{4}$$

Nodes in the same layer have the same function. Here, the output of the jth node in the layer l is $O_{l,j}$.

Layer 1. This layer node obscures the input signal.

$$O_{1,j} = \mu_{A_j}(x), j = 1, 2 \text{ or } O_{1,j} = \mu_{B_{j-2}}(x), j = 3, 4, \tag{5}$$

where x or y is the input node and $O_{1,j}$ is the membership of the fuzzy set A (A_1, A_2, B_1, or B_2). Here, the membership function of A takes a bell-shaped function, which can be represented as

$$\mu_A(x) = \frac{1}{1 + \left|x - c_j/a_j\right|^{2b_j}}, \tag{6}$$

where $\{a_j, b_j, c_j\}$ is called the antecedent parameters.

Layer 2. Multiply all input signals passed in the previous layer as the output of this layer.

$$O_{2,j} = \mu_{A_j}(x)\mu_{B_j}(y), \quad j = 1, 2. \tag{7}$$

Layer 3. The output in this layer is the normalized excitation intensity. The principle is that the jth node calculates the ratio of the excitation strength of the jth rule to the sum of the excitation strengths of all the rules.

$$O_{3,j} = \bar{w}_j = \frac{w_j}{w_1 + w_2}, \quad j = 1, 2. \tag{8}$$

Layer 4. All nodes in this layer are used as adaptive nodes with the node functions.

$$O_{4,j} = \bar{w}_j f_j = \bar{w}_j\left(p_jx + q_jy + r_j\right), \quad j = 1, 2, \tag{9}$$

where $\bar{w}_j$ is the normalized excitation intensity from the third layer and $\{p_j, q_j, r_j\}$ is the conclusion parameters or consequent parameters.

Layer 5. The last layer sums all the signals to calculate the system output.

$$O_{5,1} = \sum \bar{w}_j f_j = \frac{\sum_j w_j f_j}{\sum_j w_j}, \quad j = 1, 2. \tag{10}$$

It can be seen from the structure of ANFIS that the system has two adaptive layers (layer 1 and layer 4). The first layer has three adjustable antecedent parameters associated with the input membership functions. Layer 4 has three adjustable consequent parameters associated with the first-order polynomial. The linear combination of the consequent parameters can be used to obtain the output of ANFIS, which can be expressed as

$$\begin{aligned} f &= \bar{w}_1 f_1 + \bar{w}_2 f_2 = \bar{w}_1(p_1x + q_1y + r_1) + \bar{w}_2(p_2x + q_2y + r_2) \\ &= (\bar{w}_1 x)p_1 + (\bar{w}_1 y)q_1 + (\bar{w}_1)r_1 + (\bar{w}_2 x)p_2 + (\bar{w}_2 x)q_2 + (\bar{w}_2)r_2 \\ &= A\theta, \end{aligned} \tag{11}$$

where the elements of the column vector θ constitute a set of conclusion parameters $\{p_1, q_1, r_1, p_2, q_2, r_2\}$. If there are t groups of input and output data pairs and given the antecedent parameters, the order of the matrix A, θ, f is $t \times 6$, 6×1, and $t \times 1$, respectively. In general, the number of sample data is much larger than the number of unknown parameters, that is to say, $t>>6$. The least squares method (LSM) is used to obtain the best estimate of the conclusion parameter vector $\hat{\theta}$ in the sense of minimizing $\|A\theta - f\|^2$, namely,

$$\hat{\theta} = \left(A^TA\right)^{-1}A^Tf. \tag{12}$$

Then, based on the identification result of the conclusion parameters $\hat{\theta}$, the estimated output $\hat{f}$ of ANFIS is calculated by

$$\hat{f} = A\hat{\theta}. \tag{13}$$

The root mean square error (RMSE) under the current antecedent and conclusion parameters can be calculated by Equation (14).

$$\text{RMSE} = \sqrt{\sum_{k=1}^{t} \frac{\left(\hat{f}^k - f^k\right)^2}{t}}. \tag{14}$$

3.2. Antecedent Parameter Determination Algorithm of ANFIS. In essence, the prototype structure of ANFIS uses the mesh generation method to divide the input space by default. If the input is complex nonlinear data, it will inevitably lead to the exponential growth of the number of fuzzy rules, which will inevitably bring about dimensionality disasters. In addition, the linear division of the grid partition method cannot accurately reflect the spatial distribution of input data. Therefore, the subtraction clustering and fuzzy C-means clustering algorithms are utilized to realize the segmentation of data space and the determination of the antecedent parameters.

3.2.1. Subtractive Clustering Algorithm. In a certain group of data, each data point is regarded as a candidate point of the cluster center, and an independent and fast single-time clustering algorithm that can calculate the number of clusters and the class centers is named as the subtractive clustering method [25]. According to the subtractive clustering method, there is a simple linear relationship between the number of data points and the calculation amount, which is not

necessarily related to the dimension of the research object. Assuming that the n data points $(x_1, x_2, \cdots, x_c)$ in the M -dimensional space have been normalized to a hypercube space, the density index at the data point x_i is set as

$$D_i = \sum_{j=1}^{n} \exp\left(-\frac{\left\|x_i - x_j\right\|^2}{(r_a/2)^2}\right), \tag{15}$$

where r_a is a positive integer representing a neighborhood radius of such data points. It can be seen that a data point with multiple data points in the vicinity has a high density value, and a point outside a certain field has a minimal influence on its density index.

In the subtractive clustering algorithm, the class center may be any point. Therefore, the density index of the point and its surrounding points in the neighborhood must be calculated with each point as the class center. The possibility of this point as the class center is analyzed. After the above operations, the first class center is the point with the highest density index selected from it, which is written as x_{c1} and whose density value is D_{c1}. The corrected density index of any point $x_i (i = 1, 2, \cdots)$ can be obtained by Eq. (16).

$$D_i = D_i - D_{c1} \exp\left(-\frac{\left\|x_i - \mathrm{x}_{c1}\right\|^2}{(r_b/2)^2}\right), \tag{16}$$

where $r_b \in Z$.

Obviously, the closer the data point is to x_{c1}, the smaller the density value and then, the less likely it is a class center. In the neighborhood with radius r_b, the density value shows a decreasing trend. In general, in order to prevent the situation of the closer class centers, usually $r_b > r_a$, for example, $r_b = 1.5r_a$. After the density values of all the points are modified, the calculations of other class centers are deduced by the same method, and the density value correction is performed for all the points of the nonclass center. In this paper, the subtractive clustering method is used for pattern decomposition. Suppose the degree of the input and output belonging to a certain kind of center is $F^j(x)$ and the input set $X = \{X_1, X_2, \cdots, X_P\}$ contains p input and output data, wherein each point is expressed as

$$X^k = \left\{X_1^k, X_2^k, \cdots, X_n^k, X_{n+1}^k, \cdots, X_{n+m}^k\right\}, \tag{17}$$

where the input of the kth input and output data pair is represented as $\{X_1^k, X_2^k, \cdots, X_n^k\}$ and the corresponding output is $X_{n+1}^k, \cdots, X_{n+m}^k$.

The steps of pattern extraction based on the subtractive clustering algorithm are described as follows.

Step 1. There are p vectors $v^k, k = 1, 2, \cdots, p$, and the initial value $v^k = X^k$ is defined

Step 2. Let v^k be the reference vector and v^l be the comparison vector. Then, calculate the relationship between the two vectors

$$F^j(x) = \exp\left[\frac{-\left\|v^k - v^l\right\|^2}{\sigma_{ij}^2}\right], \tag{18}$$

where $k = 1, 2, \cdots, p$, $l = 1, 2, \cdots, p$, and $\left\|v^k - v^l\right\|^2$ indicates the Euclidean distance between the two vectors. The variance σ of the Gaussian function is calculated by the mean square error of the performance index

Step 3. Update the relationship degree between the reference vector and the comparison vector by

$$F^j(x) = \begin{cases} 0, & F^j(x) < \varepsilon, \\ F^j(x), & \text{Other}, \end{cases} \tag{19}$$

where ε is a small positive number ($\varepsilon = 0.01$)

Step 4. Calculate $\omega^k = \{\omega_1^k, \omega_2^k, \cdots, \omega_{n+m}^k\}$ by Eq. (20).

$$\omega^k = \frac{\sum_{l=1}^{p} F^j(x) v^l}{\sum_{l=1}^{p} F^j(x)}. \tag{20}$$

Step 5. When all ω^k and v^k are the same, the algorithm continues; otherwise, let $v^k = \omega^k$ and go to Step 2

Step 6. According to the final v^k obtained in the above steps, the number of clusters is equal to the number of convergence vectors. The original data with the same convergence vector is divided into one class with the convergence vector as the center

3.2.2. FCM Clustering Algorithm. The FCM clustering algorithm [26] divides the feature points in the feature space $X = (x_1, x_2, \cdots, x_n)$ into c classes $(2 \le c \le n)$, and the cluster center of the ith class is represented by v_i, where any feature point x_j belongs to the membership degree u_{ij} of the ith class, and $u_{ij} (0 \le u_{ij} \le 1)$ satisfies the following conditions.

$$\sum_{i=1}^{c} u_{ij} = 1, \quad \text{for } j = 1, 2, \cdots, n, \; 0 < \sum_{j=1}^{n} u_{ij} < n, \quad \text{for } i = 1, 2, \cdots, c. \tag{21}$$

The objective function of the FCM clustering algorithm is described as

$$J_m(U, V) = \sum_{i=1}^{c} \sum_{j=1}^{n} \left(u_{ij}\right)^m \left\|x_j - v_i\right\|^2, \tag{22}$$

where $m > 1$ is the index weight that affects the degree of fuzzification of the membership matrix. The clustering problem is to find the membership degree matrix

$U = [u_{ij}]_{c\times n}$ and the category center $V = (v_1, v_2, \cdots, v_c)$ to make Equation (3) minimized. When utilizing the FCM clustering algorithm, a parameter that needs to be determined in advance is the number of classifications of the data set. The clustering validity function used in this paper is described as follows [27].

$$V_p(U,c) = \frac{1}{n}\sum_{k=1}^{n}\max_i(u_{ik}) - \frac{1}{K}\sum_{i=1}^{c-1}\sum_{j=i+1}^{c}\left(\frac{1}{n}\sum_{k=1}^{n}\max\left(u_{ik}, u_{jk}\right)\right), \tag{23}$$

where

$$K = \sum_{i=1}^{c-1} i. \tag{24}$$

This clustering criterion combines the tightness and separation of fuzzy partitioning. By combining the clustering ISODATA algorithm with the proposed criterion function to obtain the optimal fuzzy partition, the algorithm procedure is described as follows.

Step 1. Specify the maximum number of cluster centers $c_{\max}$ ($c_{\max} \le \sqrt{n}$), the maximum number of iterations T, the index weight m, and the stop threshold $\varepsilon > 0$

Step 2. Initialize the fuzzy clustering center $V_0 = \{v_{10}, v_{20}, \cdots, v_{c0}\}$ for the number of cluster centers $c = 2, 3, \cdots, c_{\max}$

Step 3. For the number of iterations $t = 1, 2, \cdots, T$, calculate the membership matrix and cluster center according to Eq. (24) and Eq. (25).

$$u_{ij,t} = \frac{\left[1/\left\|x_i - v_j\right\|^2\right]^{1/(a-1)}}{\sum_{j=1}^{c}\left[1/\left\|x_i - v_j\right\|^2\right]^{1/(a-1)}}, \tag{25}$$

$$v_{j,t} = \frac{\sum_{i=1}^{n}\left[u_{ij,t}\right]^m x_i}{\sum_{i=1}^{n}\left[u_{ij,t}\right]^m}, \tag{26}$$

where $i = 1, 2, \cdots, n$ and $j = 1, 2, \cdots, c$. If $\|V_t - V_{t-1}\| < \varepsilon$, go to the next step; otherwise, repeat Step 3

Step 4. Calculate $V_p(U,c)$ by Equation (23). If $c < c_{\max}$, go to Step 2; otherwise, stop the iteration and output the optimal cluster number $c = c_b$, which satisfies $V_p(U,c_b) = \min\{V_p(U,c)\}$, $c = 2, 3, \cdots, c_{\max}$.

3.3. Consequent Parameter Optimization Algorithms of ANFIS

3.3.1. Gradient Algorithm. The gradient descent method, also known as the fastest descent method, is a multidimensional unconstrained optimization problem calculation method based on gradients [28]. Considering an unconstrained optimization problem,

$$\min_{x\in R^n} f(x), \tag{27}$$

where $f(x)$ has a first-order continuous partial derivative. Starting from any point $x_0 \in R^n$, the Taylor formula shows that the $f(x)$ decreases fastest along the direction of the negative gradient. Carry out the first-order Taylor spread on $f(x)$ at x along p to obtain

$$f(x+\lambda p) = f(x) + \lambda\nabla^T f(x)p + \sigma\left(\lambda^2\right), \tag{28}$$

where λ is the searching step size and p is a unit vector, that is to say, $\|p\| = 1$.

Carry out the transposition on Equation (28) to get

$$f(x+\lambda p) - f(x) = \left[\nabla^T f(x)p + \frac{o\left(\lambda^2\right)}{\lambda}\right]\lambda. \tag{29}$$

It can be seen from Equation (29) that if $\nabla^T f(x)p < 0$, there are $\bar{\lambda} > 0$ and $0 < \lambda < \bar{\lambda}$. The term of the square brackets in Equation (29) is negative, and thus, $f(x+\lambda p) < f(x)$, where p is the descending direction of $f(x)$ at x. Based on the principle of the Cauchy-Schwarz theory, obtain

$$\nabla^T f(x)p \ge -\|\nabla f(x)\| \cdot \|p\|, \tag{30}$$

$$p = -\frac{\nabla f(x)}{\|\nabla f(x)\|}. \tag{31}$$

Equation (30) is the only condition for Equation (31) to take the equal sign. For the $k+1$ iteration, get

$$x^{(k+1)} = x^{(k)} + \lambda_k p^{(k)}, \tag{32}$$

where $p^{(k)} = -\nabla f(x^{(k)})$. So, the iteration formula of the steepest descent method can be represented as

$$x^{(k+1)} = x^{(k)} - \lambda_k \nabla f\left(x^{(k)}\right), \tag{33}$$

where k is the number of iterations and λ is a constant. The expression of the Jth component in Equation (33) can be described as

$$x_j^{(k+1)} = x_j^{(k)} - \lambda_k\left(\frac{\partial f}{\partial x_j}\right). \tag{34}$$

3.3.2. Kalman Algorithm. Information fusion is the core of the Kalman algorithm [29]. The probability distribution with position as the variable obeys the Gaussian distribution, which is described as

$$p_i(x) = \frac{1}{\sigma_i\sqrt{2\pi}} \exp\left\{-\frac{(x-\bar{x})^2}{2\sigma^2}\right\} \quad (i = 1, 2). \tag{35}$$

The probability of x is proportional to $p_{12}(x) = p(x_1)$ $p(x_2)$, and the result of the product also obeys a new Gaussian distribution due to

$$\begin{aligned} p_{12}(x) &= \exp\left\{-\frac{(x-\bar{x}_1)^2}{2{\delta_1}^2} - \frac{(x-\bar{x}_2)^2}{2\delta_2^2}\right\}, \\ \frac{dp_{12}}{dx} &= -\left[\frac{\bar{x}_{12}-\bar{x}_1}{\sigma_1^2} + \frac{\bar{x}_{12}-\bar{x}_2}{\sigma_1^2}\right] \cdot p_{12}(\bar{x}_{12}) = 0. \end{aligned} \tag{36}$$

The item in parentheses is 0, so there is

$$\bar{x}_{12} = \left\{\frac{\sigma_2^2}{\sigma_1^2+\sigma_2^2}\right\}x_1 + \left\{\frac{\sigma_1^2}{\sigma_1^2+\sigma_2^2}\right\}x_2. \tag{37}$$

Substitute the mean into $p(x_{12})$ to get

$$\sigma_{12}^2 = \frac{\sigma_1^2\sigma_2^2}{\sigma_1^2+\sigma_2^2}. \tag{38}$$

The above description can convert two Gaussian distributions into one Gaussian distribution. When there are multiple Gaussian distributions, they can be merged one by one. So the $\hat{x}_1 = x_1$ and $\hat{\sigma}_1^2 = \sigma_1^2$ can be replaced with the optimal estimate, that is to say,

$$\begin{aligned} \bar{x}_2 &= \frac{\sigma_2^2}{\hat{\sigma}_1^2+\sigma_2^2}x_1 + \frac{\sigma_1^2}{\hat{\sigma}_1^2+\sigma_2^2}x_2, \\ \hat{x}_2 &= \hat{x}_1 + \frac{\hat{\sigma}_1^2}{\hat{\sigma}_1^2+\sigma_2^2}(x_2 - \hat{x}_1). \end{aligned} \tag{39}$$

There are also $\hat{\sigma}_1^2 = \sigma_1^2$ and $\hat{\sigma}_2^2 = \sigma_2^2\hat{\sigma}_1^2/(\hat{\sigma}_1^2+\sigma_2^2)$. Arrange the equations to obtain a new covariance formula:

$$\hat{\sigma}_2^2 = \left(1 - \frac{\hat{\sigma}_1^2}{\hat{\sigma}_1^2+\sigma_2^2}\right)\hat{\sigma}_1^2. \tag{40}$$

Iteratively update the scale factor K by Equation (41).

$$K = \frac{\hat{\sigma}_1^2}{\hat{\sigma}_1^2+\sigma_2^2}. \tag{41}$$

Feed K into the mean to get

$$\hat{x}_2 = \hat{x}_1 + K(x_2 - \hat{x}_1) \tag{42}$$

Bring K into the covariance formula to obtain

$$\hat{\sigma}_1^2 = (1-K)\hat{\sigma}_1^2. \tag{43}$$

3.3.3. Kaczmarz Algorithm. The basic principle of the Kaczmarz algorithm is described as follows [30]. Let the map f_i from R^n to R^n be defined as

$$f_i(x) = x - \frac{(x, a_i) - b_i}{\|a_i\|_2^2}a^i, \quad i = 1, 2, \cdots, m. \tag{44}$$

The mapping from R^{m+n} to R^n can be defined as

$$F(b, x) = f_1 \circ f_2 \circ \cdots \circ f_m(x) = f_1(f_2(f_3(\cdots(f_m(x))\cdots))). \tag{45}$$

Optionally select $x^{(0)} = R^n$ and calculate the iterative sequence $\{x^{(i)}\}$ by utilizing the recursive formula.

$$x^{(i+1)} = F\left(b, x^{(i)}\right), \quad i = 0, 1, 2, \cdots, \tag{46}$$

where F is defined by Equations (44) and (45).

The orthogonal projection P_i from R^n to the Ith plane $\langle a_i, x\rangle = 0$ can be defined as

$$p_i = I - \frac{1}{\|a_i\|_2^2}a_i a_i^T = \delta_{kl} - \frac{a_{ik}a_{il}}{\|a_i\|_2^2}. \tag{47}$$

So the mapping shown in Equation (47) is then expressed as

$$f_i(x) = P_i x + \frac{b_i}{\|a_i\|_2^2}a_i, \quad i = 1, 2, \cdots, m. \tag{48}$$

Let $Q_i = P_1P_2 \cdots P_i (i = 1, 2, \cdots, m)$, where $Q_0 = I$, and matrix R satisfies the following relationship:

$$Rb = \sum_{i=1}^{m} \frac{b_i}{\|a_i\|_2^2} Q_{i-1}a_i. \tag{49}$$

According to the above equations, the expression of $F(b, x)$ can be deduced.

$$F(b, x) = Qx + Rb, \tag{50}$$

where $Q = Q_m$, and matrix R depends on matrix A. Based on Equations (49) and (50), the Kaczmarz iterative may be described as

$$x^{(i)} = Q^i x^{(0)} + \left(\sum_{j=0}^{i-1} Q^j R\right)b. \tag{51}$$

Let $\tilde{Q} = QP_{R(A^T)}$, where $P_{R(A^T)}$ is the orthogonal projection from R^n to $R(A^T)$. Then, define

$$G = \left(I - \tilde{Q}\right)^{-1} R. \tag{52}$$

Based on Equation (52), matrix G has the following property:

$$\begin{aligned} AGA &= A, \\ GAG &= G, \\ GA &= P_{R\left(A^T\right)}, \\ AG &= P, \end{aligned} \tag{53}$$

where P is a projection along $N(R)$ to $R(A)$ and $GA = P_{R(A^T)}$, which can be replaced by $(GA)^T = GA$.

3.3.4. PseudoInv Algorithm. The PseudoInv algorithm is implemented using the Moore-Penrose generalized inverse [31]. It is often applied to obtain the least norm least squares solution (least squares method) on the nonuniform linear equations and makes the form of the solution simple. The Moore-Penrose generalized inverse of the matrix is unique in both the real and complex domains and can be obtained by the singular value decomposition. The pseudoinverse of matrix A can be defined as

$$A^+ = \lim_{a \to 0} \left(A^T A + \alpha I\right)^{-1} A^T. \tag{54}$$

The actual algorithm for calculating the pseudoinverse adopts Eq. (55).

$$A^+ = V D^+ U^T. \tag{55}$$

When the number of columns of matrix A is more than the number of rows, solving the linear equation using pseudoinverse is one of the many possible solutions. Specifically, $x = A^+ y$ is $|x|_2$ with the smallest Euclidean norm in all feasible solutions for this equation. When the number of rows in matrix A is more than the number of columns, there may be no solution. In this case, x obtained by pseudoreverse is a solution that minimizes the Euclidean distance $|Ax - y|_2$ of Ax and y.

4. Simulation Experiment and Result Analysis

Based on the technique of the SMB chromatographic separation process, a soft sensor model on the target purity of E and R ports is proposed by utilizing ANFIS. The ANFIS network has three input variables and one output variable. The historical data of the SMB chromatographic separation process was collected, and 1000 sets of historical data with uniformity and representative were selected. Then, the processed data is divided into two parts. The first 800 sets of data are used as training data, and the last 200 sets of data are used to verify the performance of the soft sensor models. According to the reference data, it can be found that the target purity in the E effluent and the yield of the impurity at the R port are correlated, and the impurity purity in the R effluent and the yield of the target at the E port are also correlated. Therefore, in the experimental simulation stage, the target purity in the E effluent and the impurity purity in the R effluent are selected as the output. In order to measure the performance of the predictive models, several performance indicators are defined below, where $\hat{y}$ is the estimated value and y is the actual value [32]. The model performance indicators are defined as shown in Table 2.

Table 2: Definition of model performance indicators.

Root mean square error (RMSE)	$\mathrm{RMSE} = \left[1/n \sum_{i=1}^{n} (y\wedge_i - y_i)^2\right]^{1/2}$
Sum of squared errors (SSE)	$\mathrm{SSE} = \sum_{i=1}^{n} (y\wedge_i - y_i)^2$
Mean absolute percentage error (MAPE)	$\mathrm{MAPE} = \sum(\lvert\hat{y}_i - y_i\rvert / y_i) \times 100/n$
Maximum positive error (MPE)	$\mathrm{MPE} = \max\{(\hat{y} - y), 0\}$

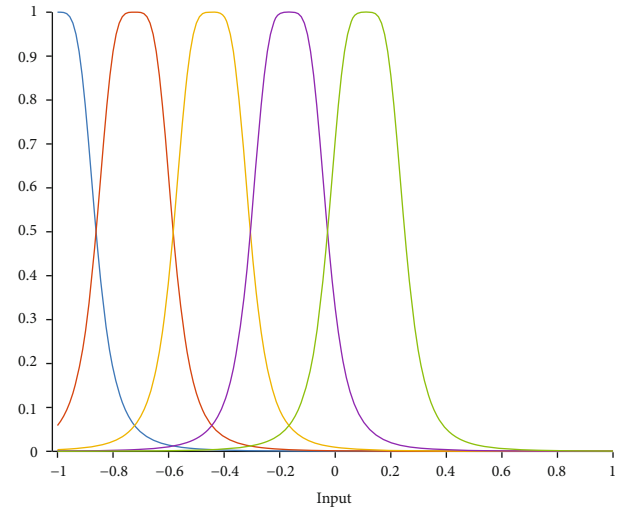

Figure 4: Input membership function based on the meshing partition method.

Based on the meshing partition method, subtractive clustering algorithm, and FCM clustering algorithm, the input data space of the SMB chromatographic separation process is divided and the premise parameters are determined. The Sugeno-type ANFIS soft sensor models based on three algorithms are established. Then, these models are optimized by the gradient, Kalman, Kaczmarz, and PseudoInv algorithms to obtain the optimized conclusion parameters so as to achieve the prediction of the target purity of the E port and R port in the SMB chromatographic separation process.

4.1. ANFIS Soft Sensor Model Based on Mesh Partition. When the input data space of the soft sensor model is divided by the meshing partition method, the membership function selects the Gaussian function, and the number of membership functions is 5. The membership function curves of the input data of the Sugeno-type ANFIS model based on meshing partition are shown in Figure 4. The number

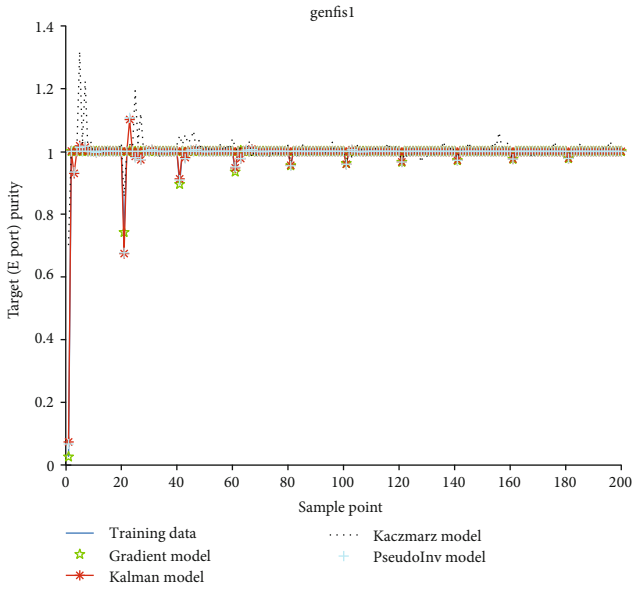

Figure 5: Effluent purity prediction results in the E port.

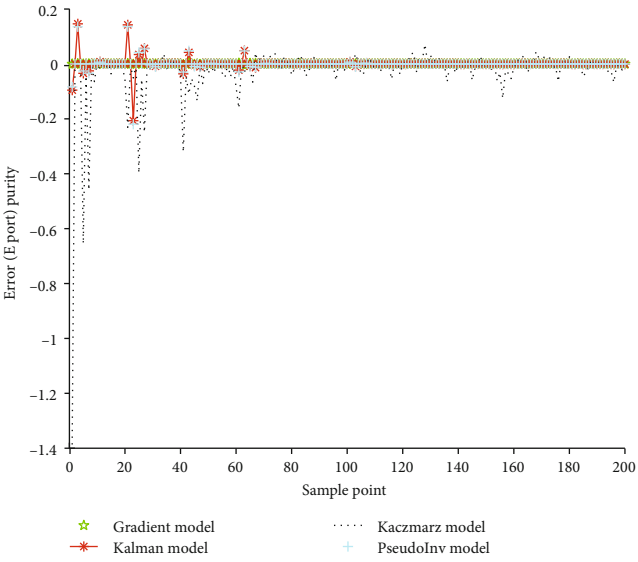

Figure 6: Effluent purity prediction error in the E port.

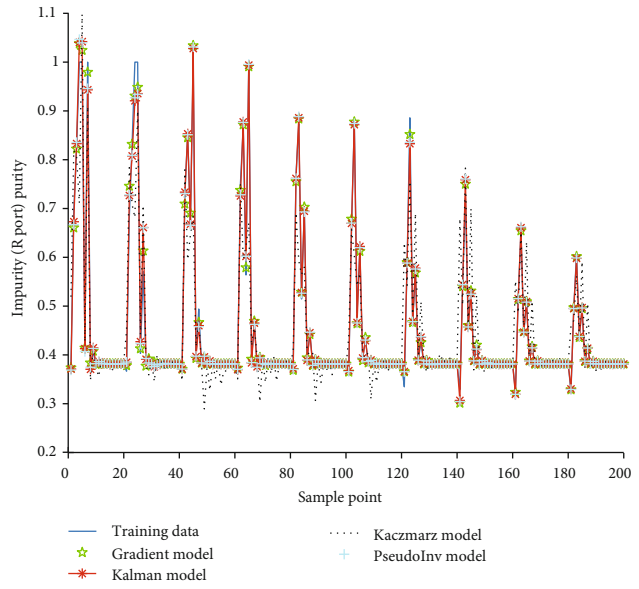

Figure 7: Prediction results of impurity purity in the R port.

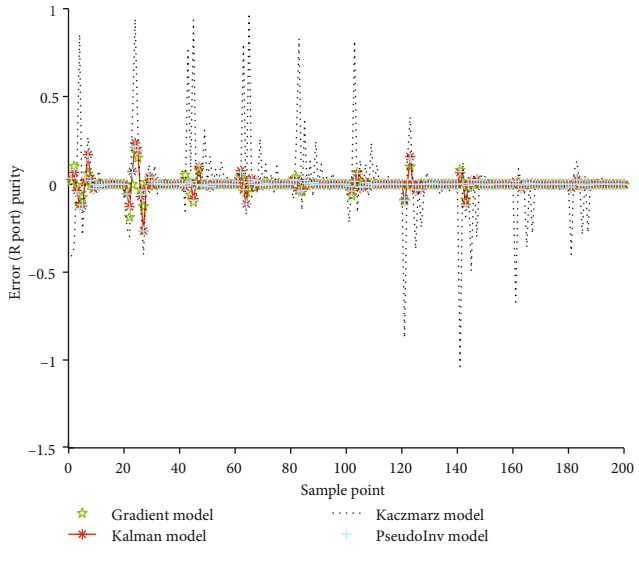

Figure 8: Prediction error of impurity purity in the R port.

of training iterations is 500, and the established soft sensor models are tested by the utilized 200 sets of data with average and representative. The predicted simulation results are shown in Figures 5–8. Figure 5 shows the output contrast of the target purity in the E port effluent in the SMB chromatography process under the gradient, Kalman, Kaczmarz, and PseudoInv algorithms to obtain the optimized conclusion parameters of ANFIS. Figure 6 shows the predictive error comparison curves. Figure 7 shows the output contrast of the impurity purity in the R port effluent in the SMB chromatography process under the gradient, Kalman, Kaczmarz, and PseudoInv algorithms to obtain the optimized conclusion parameters of ANFIS. Figure 8 shows the predictive error comparison curves. Table 3 compares the predicted performance indicators of the established soft sensor models.

According to the above simulation results, it can be seen that the input data spatial division and premise parameter determination are realized by the meshing partition method and ANFIS soft sensor models based on the gradient, Kalman, and PseudoInv algorithms for optimizing conclusion parameters have the better prediction results on the key economic and technical indicators of the SMB chromatographic separation process. In order to distinguish the optimization performance of the four algorithms, based on the adopted four performance indicators (RMSE, SSE, MAPE, and MPE), the ANFIS soft sensor model based on the meshing partition method and

Table 3: Comparison of predictive performance indicators of the ANFIS soft sensor model based on the meshing partition method.

Performance		RMSE	SSE	MAPE	MPE
Purity of the E port	Gradient	$3.3668e-04$	$2.2670e-05$	0.0081	0.0026
	Kalman	0.0112	0.0252	0.0087	0.1010
	Kaczmarz	0.0612	0.7484	0.0337	0.6750
	PseudoInv	0.0112	0.0250	0.0087	0.1068
Purity of the R port	Gradient	0.0114	0.0421	0.5512	0.0691
	Kalman	0.0145	0.0421	0.5513	0.0900
	Kaczmarz	0.0797	1.2699	0.5932	0.3585
	PseudoInv	0.0145	0.0418	0.5516	0.0896

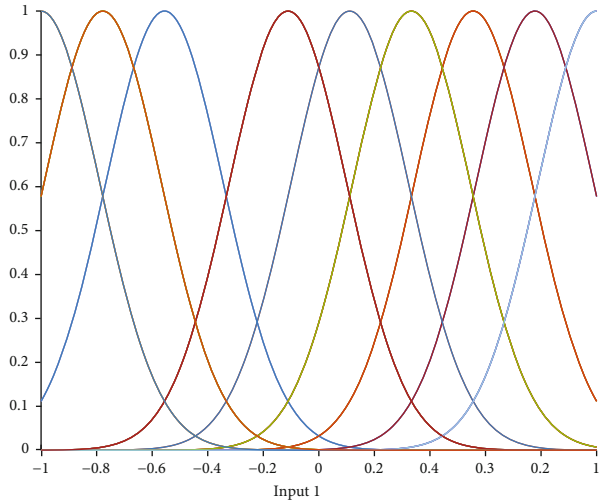

Figure 9: Membership function of input 1 based on the subtractive clustering method.

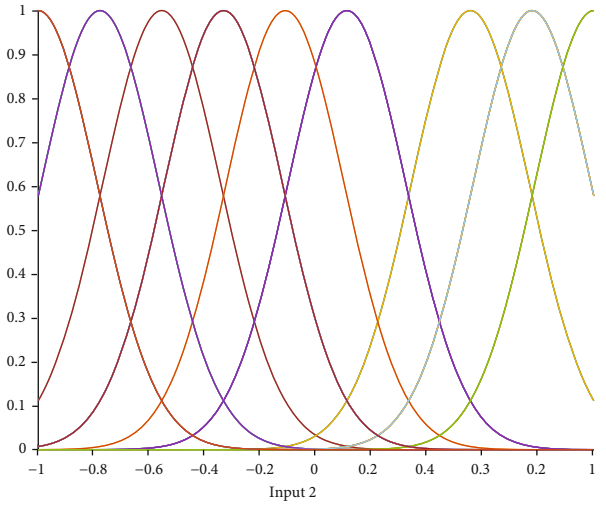

Figure 10: Membership function of input 2 based on the subtractive clustering method.

the gradient algorithm has higher prediction accuracy than the other three algorithms.

4.2. ANFIS Soft Sensor Model Based on the Subtractive Clustering Algorithm. When the input data space of the soft sensor model is divided by the subtractive clustering algorithm, the membership function selects the Gaussian function. The membership function curves of the input data of the Sugeno-type ANFIS model based on the subtractive clustering algorithm are shown in Figures 9–11. The number of training iterations is 500, and the established soft sensor models are tested by the utilized 200 sets of data with average and representative. The predicted simulation results are shown in Figures 12–15. Figure 12 shows the output contrast of the target purity in the E port effluent in the SMB chromatography process under the gradient, Kalman, Kaczmarz, and PseudoInv algorithms to obtain the optimized conclusion parameters of ANFIS. Figure 13 shows the predictive error comparison curves. Figure 14 shows the output contrast of the impurity purity in the R port effluent in the SMB chromatography process under the gradient, Kalman, Kaczmarz, and PseudoInv algorithms to obtain the optimized conclusion parameters of ANFIS. Figure 15 shows

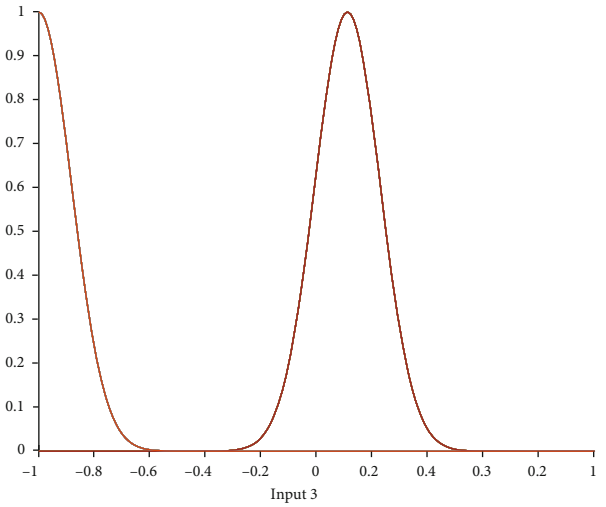

Figure 11: Membership function of input 3 based on the subtractive clustering method.

the predictive error comparison curves. Table 4 compares the predicted performance indicators of the established soft sensor models.

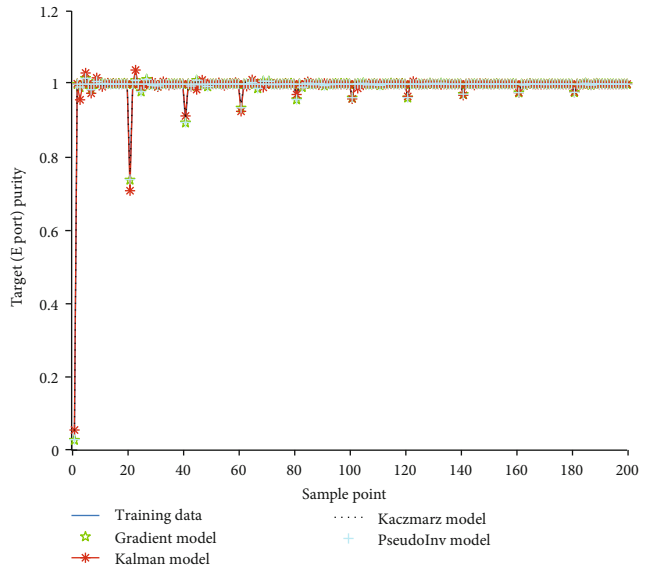

Figure 12: Effluent purity prediction results in the E port.

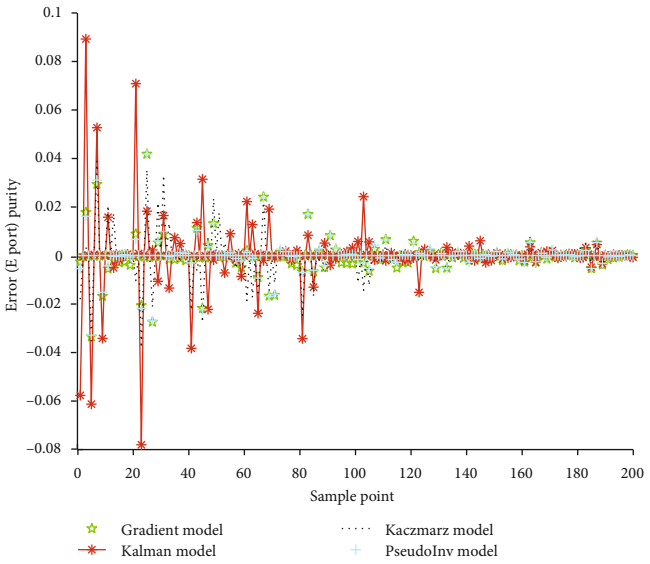

Figure 13: Effluent purity prediction error in the E port.

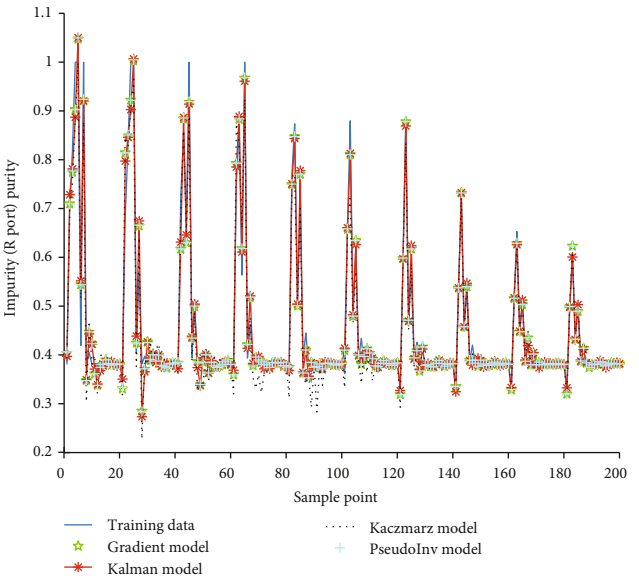

Figure 14: Prediction results of impurity purity in the R port.

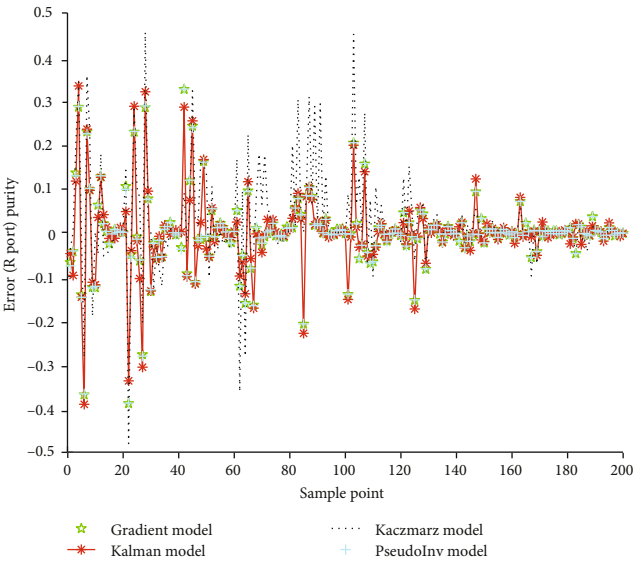

Figure 15: Prediction error of impurity purity in the R port.

According to the above simulation results, it can be seen that the input data spatial division and premise parameter determination are realized by the subtractive clustering algorithm and ANFIS soft sensor models based on the gradient, Kalman, and PseudoInv algorithms for optimizing conclusion parameters have the better prediction results on the key economic and technical indicators of the SMB chromatographic separation process. In order to distinguish the optimization performance of the four algorithms, based on the adopted four performance indicators (RMSE, SSE, MAPE, and MPE), the ANFIS soft sensor model based on the meshing partition method and the PseudoInv algorithm has higher prediction accuracy than the other three algorithms.

Table 4: Comparison of predictive performance indicators of the ANFIS soft sensor model based on the subtractive clustering method.

Performance		RMSE	SSE	MAPE	MPE
Purity of the E port	Gradient	0.0032	0.0021	0.0103	0.0204
	Kalman	0.0068	0.0092	0.0091	0.0434
	Kaczmarz	0.0042	0.0035	0.0093	0.0189
	PseudoInv	0.0032	0.0020	0.0097	0.0203
Purity of the R port	Gradient	0.0280	0.1567	0.5517	0.1315
	Kalman	0.0286	0.1633	0.5514	0.5514
	Kaczmarz	0.0386	0.2981	0.5809	0.1624
	PseudoInv	0.0280	0.1566	0.5515	0.1313

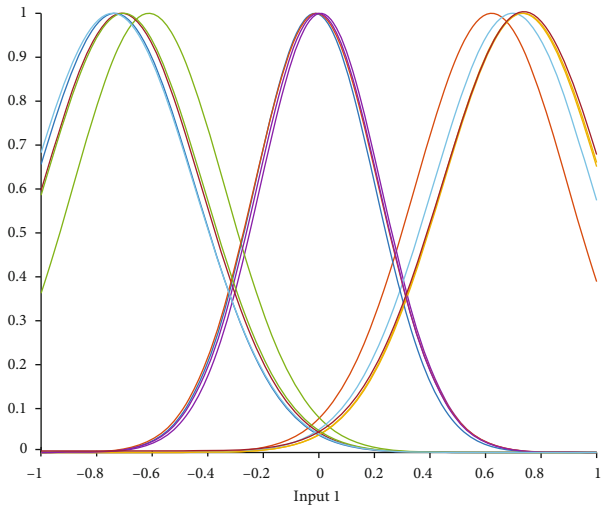

Figure 16: Membership function of input 1 based on the FCM clustering method.

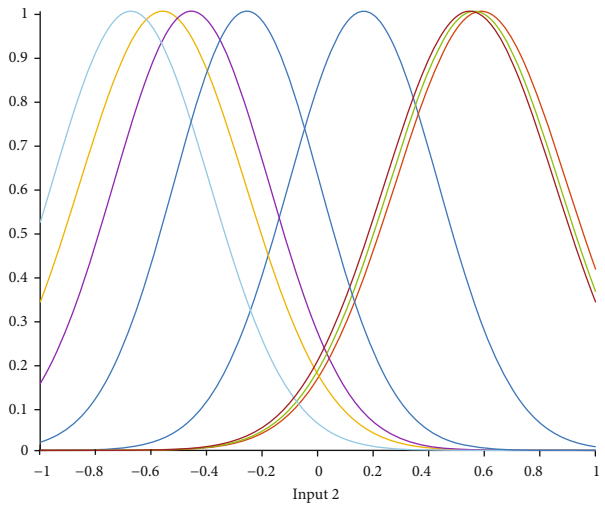

Figure 17: Membership function of input 2 based on the FCM clustering method.

4.3. ANFIS Soft Sensor Model Based on the FCM Clustering Algorithm. When the input data space of the soft sensor model is divided by the FCM clustering algorithm, the membership function selects the Gaussian function. The membership function curves of the input data of the Sugeno-type ANFIS model based on the FCM clustering algorithm are shown in Figures 16–18. The number of training iterations is 500, and the established soft sensor models are tested by the utilized 200 sets of data with average and representative. The predicted simulation results are shown in Figures 19–22. Figure 19 shows the output contrast of the target purity in the E port effluent in the SMB chromatography process under the gradient, Kalman, Kaczmarz, and PseudoInv algorithms to obtain the optimized conclusion parameters of ANFIS. Figure 20 shows the predictive error comparison curves. Figure 21 shows the output contrast of the impurity purity in the R port effluent in the SMB chromatography process under the gradient, Kalman, Kaczmarz, and PseudoInv

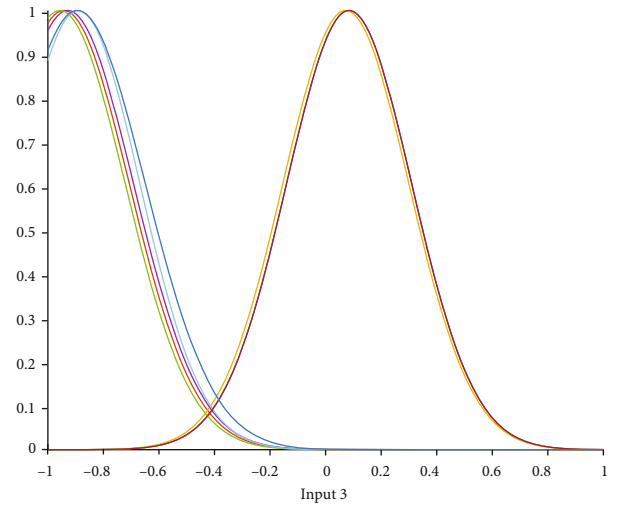

Figure 18: Membership function of input 3 based on the FCM clustering method.

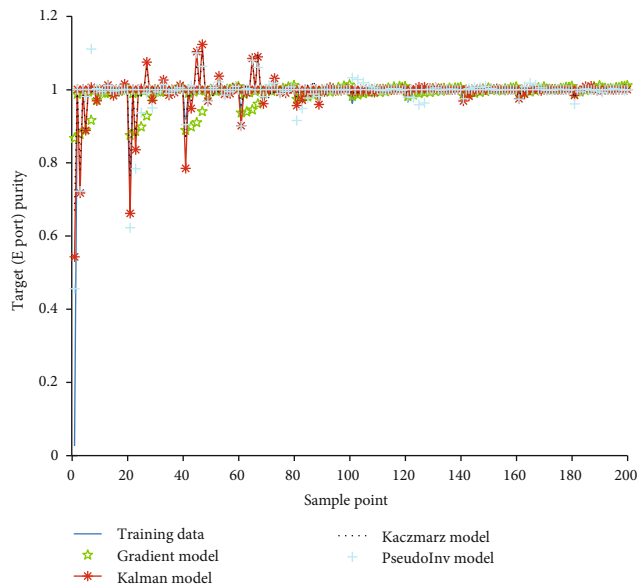

Figure 19: Effluent purity prediction results in the E port.

algorithms to obtain the optimized conclusion parameters of ANFIS. Figure 22 shows the predictive error comparison curves. Table 5 compares the predicted performance indicators of the established soft sensor models.

According to the above simulation results, it can be seen that the input data spatial division and premise parameter determination are realized by utilizing the FCM clustering algorithm and ANFIS soft sensor models based on the Kalman, Kaczmarz, and PseudoInv algorithms for optimizing conclusion parameters have the better prediction results on the key economic and technical indicators of the SMB chromatographic separation process. In order to distinguish the optimization performance of the four algorithms, based on the adopted four performance indicators (RMSE, SSE, MAPE, and MPE), the ANFIS soft sensor model based on the FCM clustering algorithm and the

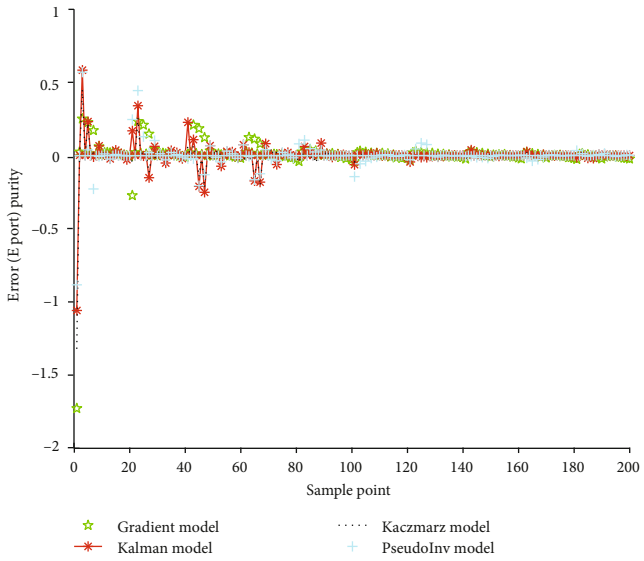

Figure 20: Effluent purity prediction error in the E port.

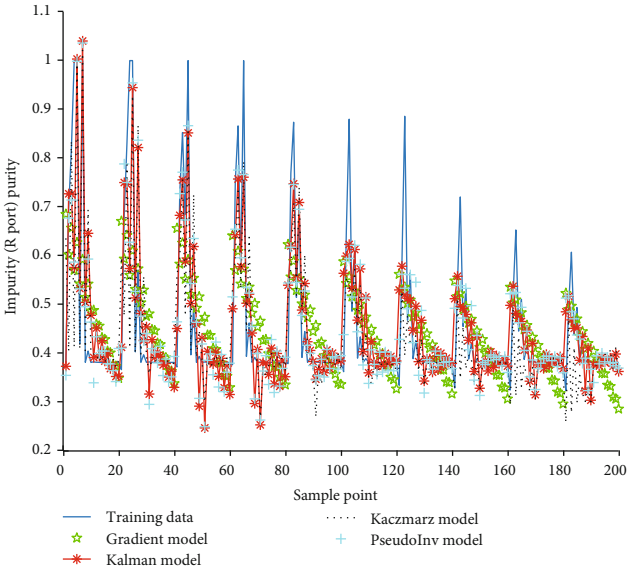

Figure 21: Prediction results of impurity purity in the R port.

PseudoInv algorithm has higher prediction accuracy than the other three algorithms.

5. Conclusions

In this paper, a soft sensing modeling method of the SMB chromatographic separation process based on ANFIS is proposed. Three input data space division and antecedent parameter determination methods are combined with four consequent parameter optimization algorithms to realize the ANFIS soft sensing models on the target purity of the E port and R port in the SMB chromatographic separation process. The simulation results verify that the proposed models can obtain better prediction results on the

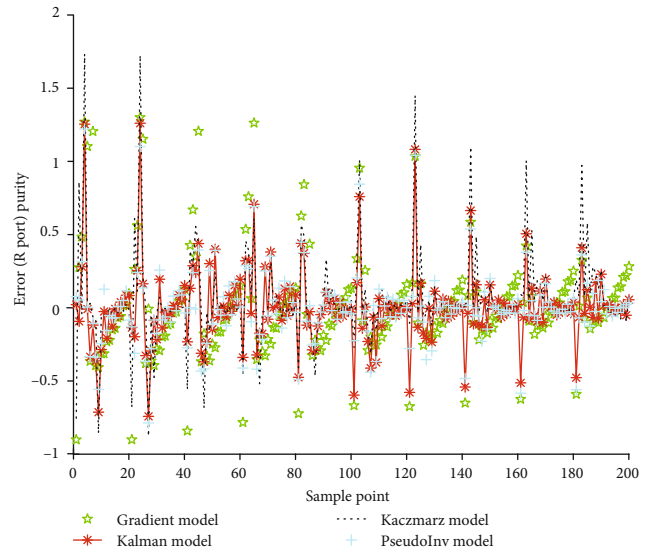

Figure 22: Prediction error of impurity purity in the R port.

Table 5: Comparison of predictive performance indicators of the ANFIS soft sensor model based on the FCM clustering method.

Performance		RMSE	SSE	MAPE	MPE
Purity of the E port	Gradient	0.0643	0.8281	0.0258	0.8410
	Kalman	0.0485	0.4699	0.0258	0.5163
	Kaczmarz	0.0517	0.5344	0.0196	0.6431
	PseudoInv	0.0440	0.3874	0.0253	0.4297
Purity of the R port	Gradient	0.1245	3.0982	0.5547	0.4398
	Kalman	0.087	1.5336	0.5557	0.4262
	Kaczmarz	0.1131	2.5603	0.6397	0.5862
	PseudoInv	0.0837	1.4009	0.5558	0.4129

purity of components, which will supply the foundation of the quality closed-loop control.

Data Availability

There are no data available for this paper.

Conflicts of Interest

The authors declare no conflict of interest.

Authors' Contributions

Dan Wang participated in the algorithm simulation and draft writing. Jie-Sheng Wang participated in the concept, design, and critical revision of this paper. Shao-Yan Wang participated in the interpretation and commented on the manuscript. Shou-Jiang Li participated in the SMB chromatographic separation process technique. Zhen Yan participated in the data collection and analysis. Wei-Zhen Sun participated in the simulation methods.

Acknowledgments

This work is partially supported by the project of National Natural Science Foundation of China (Grant No. 21576127), the Basic Scientific Research Project of Institution of Higher Learning of Liaoning Province (Grant No. 2017FWDF10), and the project of Liaoning Provincial Natural Science Foundation of China (Grant No. 20180550700).

References

[1] Y. I. Lim and S. B. Jorgensen, "A fast and accurate numerical method for solving simulated moving bed (SMB) chromatographic separation problems," *Chemical Engineering Science*, vol. 59, no. 10, pp. 1931–1947, 2004.

[2] S. F. Brown, M. D. Ogden, and E. S. Fraga, "Efficient simulation of chromatographic separation processes," *Computers & Chemical Engineering*, vol. 110, pp. 69–77, 2018.

[3] K. M. Kim, W. L. Ju, S. Kim, F. V. S. da Silva, A. Seidel-Morgenstern, and C.-H. Lee, "Advanced operating strategies to extend the applications of simulated moving bed chromatography," *Chemical Engineering & Technology*, vol. 40, no. 12, pp. 2163–2178, 2017.

[4] L. Ling, Y. Decheng, and J. Yuanwei, "Research on soft measurement modeling and simulation of simulated moving bed process," *Computers and Applied Chemistry*, vol. 31, no. 11, pp. 1298–1302, 2014.

[5] J. S. R. Jang, "ANFIS: adaptive-network-based fuzzy inference system," *IEEE Transactions on Systems Man and Cybernetics*, vol. 23, no. 3, pp. 665–685, 1993.

[6] J. P. S. Catalao, H. M. I. Pousinho, and V. M. F. Mendes, "Hybrid wavelet-PSO-ANFIS approach for short-term electricity prices forecasting," *IEEE Transactions on Power Systems*, vol. 26, no. 1, pp. 137–144, 2011.

[7] I. Yilmaz and O. Kaynar, "Multiple regression, ANN (RBF, MLP) and ANFIS models for prediction of swell potential of clayey soils," *Expert Systems with Applications*, vol. 38, no. 5, pp. 5958–5966, 2011.

[8] M. Mohandes, S. Rehman, and S. M. Rahman, "Estimation of wind speed profile using adaptive neuro-fuzzy inference system (ANFIS)," *Applied Energy*, vol. 88, no. 11, pp. 4024–4032, 2011.

[9] M. Talebizadeh and A. Moridnejad, "Uncertainty analysis for the forecast of lake level fluctuations using ensembles of ANN and ANFIS models," *Expert Systems with Applications*, vol. 38, no. 4, pp. 4126–4135, 2011.

[10] I. Maher, L. H. Ling, A. A. D. Sarhan, and M. Hamdi, "Improve wire EDM performance at different machining parameters - ANFIS modeling," *IFAC PapersOnline*, vol. 48, no. 1, pp. 105–110, 2015.

[11] A. Najafi-Marghmaleki, A. Barati-Harooni, and A. H. Mohammadi, "ANFIS modeling of ionic liquids densities," *Journal of Molecular Liquids*, vol. 224, Part A, pp. 965–975, 2016.

[12] M. Y. Chen, "A hybrid ANFIS model for business failure prediction utilizing particle swarm optimization and subtractive clustering," *Information Sciences*, vol. 220, no. 1, pp. 180–195, 2013.

[13] K. Mohammad, R. S. Vali, A. C. Reza, E. Taghinezhad, Y. Abbaspour-Gilandeh, and I. Golpour, "ANFIS and ANNs model for prediction of moisture diffusivity and specific energy consumption potato, garlic and cantaloupe drying under convective hot air dryer," *Information Processing in Agriculture*, vol. 5, no. 3, pp. 372–387, 2018.

[14] A. Gholami, H. Bonakdari, I. Ebtehaj, S. H. A. Talesh, S. R. Khodashenas, and A. Jamali, "Analyzing bank profile shape of alluvial stable channels using robust optimization and evolutionary ANFIS methods," *Applied Water Science*, vol. 9, no. 3, 2019.

[15] K. Siddharth, A. Pathak, and A. K. Pani, "Real-time quality monitoring in debutanizer column with regression tree and ANFIS," *Journal of Industrial Engineering International*, vol. 15, no. 1, pp. 41–51, 2019.

[16] E. Soroush, M. Mesbah, N. Hajilary, and M. Rezakazemi, "ANFIS modeling for prediction of CO_2 solubility in potassium and sodium based amino acid salt solutions," vol. 7, no. 1, Article ID 102925, 2019Journal of Environmental Chemical Engineering.

[17] M. Rezakazemi and S. Shirazian, "Gas-liquid phase recirculation in bubble column reactors: development of a hybrid model based on local CFD – adaptive neuro-fuzzy inference system (ANFIS)," *Journal of Non-Equilibrium Thermodynamics*, vol. 44, no. 1, 2019.

[18] I. Shivakoti, G. Kibria, P. M. Pradhan, B. B. Pradhan, and A. Sharma, "ANFIS based prediction and parametric analysis during turning operation of stainless steel 202," *Materials and Manufacturing Processes*, vol. 34, no. 1, 2019.

[19] Y. Z. And and P. C. Wankat, "SMB operation strategy−partial feed," *Industrial & Engineering Chemistry Research*, vol. 41, no. 10, pp. 2504–2511, 2002.

[20] F. He, *Modeling and optimization of simulated moving bed chromatography separation process*, Jiangnan University, 2002.

[21] G. M. Zhong and G. G. Chon, "Analytical solution for the linear ideal model of simulated moving bed chromatography," *Chemical Engineering Science*, vol. 51, no. 18, pp. 4307–4319, 1996.

[22] M. S. G. García, E. Balsa-Canto, A. V. Wouwer, and J. R. Banga, "Optimal control of the simulated moving bed (SMB) chromatographic separation process," *IFAC Proceedings Volumes*, vol. 40, no. 5, pp. 183–188, 2007.

[23] P.-C. Chang and C.-H. Liu, "A TSK type fuzzy rule based system for stock price prediction," *Expert Systems with Applications*, vol. 34, no. 1, pp. 135–144, 2008.

[24] J.-s. Wang and C.-x. Ning, "ANFIS based time series prediction method of bank cash flow optimized by adaptive population activity PSO algorithm," *Information*, vol. 6, no. 3, pp. 300–313, 2015.

[25] M. Ghane'i-Ostad, H. Vahdat-Nejad, and M. Abdolrazzagh-Nezhad, "Detecting overlapping communities in LBSNs by fuzzy subtractive clustering," *Social Network Analysis and Mining*, vol. 8, no. 1, p. 23, 2018.

[26] J. C. Bezdek, R. Ehrlich, and W. Full, "FCM: The fuzzy *c*-means clustering algorithm," *Computers & Geosciences*, vol. 10, no. 2-3, pp. 191–203, 1984.

[27] K. L. Wu, M. S. Yang, and J. N. Hsieh, "Robust cluster validity indexes," *Pattern Recognition*, vol. 42, no. 11, pp. 2541–2550, 2009.

[28] K.-C. Toh and S. Yun, "An accelerated proximal gradient algorithm for nuclear norm regularized least squares problems," *Pacific Journal of Optimization*, vol. 6, no. 3, pp. 615–640, 2010.

[29] D. Panigrahy and P. K. Sahu, "Extraction of fetal electrocardiogram (ECG) by extended state Kalman filtering and adaptive

neuro-fuzzy inference system (ANFIS) based on single channel abdominal recording," *Sadhana*, vol. 40, no. 4, pp. 1091–1104, 2015.

[30] L. Dai, M. Soltanalian, and K. Pelckmans, "On the randomized Kaczmarz algorithm," *IEEE Signal Processing Letters*, vol. 21, no. 3, pp. 330–333, 2014.

[31] T. Górecki and M. Łuczak, "Linear discriminant analysis with a generalization of the Moore–Penrose pseudoinverse," *International Journal of Applied Mathematics & Computer Science*, vol. 23, no. 2, pp. 463–471, 2013.

[32] W. Z. Sun and J. S. Wang, "A Universal Predictive Mobility Management Scheme for Urban Ultra-dense Networks with Control/Data Plane Separation," *IEEE Access*, vol. 5, pp. 6015–6026, 2017.